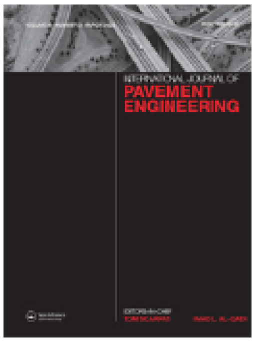

International Journal of Pavement Engineering

ISSN: (Print) (Online) Journal homepage: https://www.tandfonline.com/loi/gpav20

Rigid pavement icing: misting tests on a model pavement column under simulated cold fronts inside a freezer

Taryn DiLorenzo, Omid Habibzadeh-Bigdarvish, Dongfeng Li, Zheng Fang, Andrew Kruzic & Xinbao Yu

INTERNATIONAL JOURNAL OF PAVEMENT ENGINEERING
https://doi.org/10.1080/10298436.2022.2044036

RESEARCH ARTICLE

Rigid pavement icing: misting tests on a model pavement column under simulated cold fronts inside a freezer

Taryn DiLorenzo, Omid Habibzadeh-Bigdarvish, Dongfeng Li, Zheng Fang, Andrew Kruzic and Xinbao Yu

Department of Civil Engineering, University of Texas at Arlington, Arlington, USA

Abstract

Meteorological and subsurface factors influence pavement's response to cold fronts. Prediction of pavement temperature, particularly icing, is important to winter pavement maintenance which relies on an estimated time for the formation of ice. However, the prediction development is limited by test data on pavement icing. A model column consisting of soil samples and a concrete pavement slab retrieved from the Dallas Fort Worth airport was used to replicate the airport pavement structure, including subgrade. The soil was classified using USCS, tested for optimum moisture content and compacted in lifts in the column. Thermistors and moisture sensors were placed at different depths. The pavement slab was fitted with temperature sensors throughout. The system was installed in a freezer box,wrapped in insulation and plastic. Three cold front scenarios were selected from observed airport weather data and simulated in the freezer box using varying rates of temperature decrease and precipitation. The formation of ice on a pavement surface was observed at 10–20 min after the start of precipitation. This time frame is not affected by the freezer box cooling rate. The icing time found from this study is useful for the development of prediction models for icing onpavements.

ARTICLE HISTORY
Received 3 November 2021
Accepted 14 February 2022

Keywords
Pavement temperature; icing time; cold front

1 Introduction

The correlation of meteorological data and pavement conditions is crucial for winter pavement maintenance. It determines how pavement responds to cold fronts and when the formation of icing can be expected. More than 70 percent of the roadways in the United States are in areas affected by adverse winter weather. Vehicle crashes due to icy pavement conditions account for 24 percent of accidents annually, with 15 percent of those accidents occurring during a winter precipitation event. Adverse road conditions increase travel time and fuel consumption while decreasing profits for businesses. The cost for maintaining roads in the winter is estimated to be 20 percent of local Department of Transportation (DOT) annual budgets (Snow & Ice- FHWA Road Weather Managment 2020), this includes a direct cost of 2.3 billion dollars and an infrastructure cost of approximately 5 billion dollars (Veneziano *et al.* 2018). Chemicals used in winter road maintenance can have negative effects on soil and water as well as vegetation and wildlife in the form of runoff (Dai *et al.* 2012, Usman *et al.* 2012). The negative impacts of chemicals and abrasives are not just limited to the natural environment. Bridges, pavements, and vehicles can also be damaged by the corrosion caused by reactive winter pavement maintenance (Sutter *et al.* 2006).

The ability to predict pavement temperature response ahead of a winter event can mitigate many of the negative effects of adverse road conditions through the proactive approach of applying anti-icing (O'Keefe and Shi 2005). DOTs will pretreat roads and bridges ahead of time when the weather forecast predicts freezing temperatures along with precipitation. The pavement temperature response is applicable not only for roadway maintenance but also pavement design, analysis of urban heat island effect, and the research and development of new pavement materials. There have been numerous studies and modelings on the pavement temperature response in field conditions that predict pavement surface temperature based on collected field data (Chen *et al.* 2019, Qiu *et al.* 2018, Zhao *et al.*, 2020). The pavement temperature prediction has been generally studied in the field under dry conditions, neglecting the effects of precipitation and the associated phase changes. The temperature response due to precipitation has not been widely studied. Pavement surface icing has been studied using meteorological sensors in the field where conditions cannot be controlled. As a result, these studies lack repeatability. There is also a lack of experimental studies on pavement response performed under controlled conditions that consider both the meteorological factors and the soil temperature (Chen *et al.* 2019).

The aim of this study is to measure the pavement temperature inside a model pavement column tested inside a freezer box under controlled weather scenarios. The objectives are to determine the lead time for the formation of ice and to explore how the soil's thermal capacity affects the pavement response to cold fronts. In this study, a pavement model column was designed, built, and installed into a freezer box to observe the temperature response of both the pavement and the subsurface soil to simulated cold fronts of varying duration and intensity. A misting system installed in the freezer box was used for simulated precipitation events to observe the conditions required for the potential of ice formation. Sensors were installed in the soil to record temperature and moisture. Sensors in the pavement slab recorded surface and pavement

CONTACT Xinbao Yu xinbao@uta.edu

body temperature. The ambient temperature and the relative humidity of the freezer box environment were recorded as well.

2 Materials and methods

2.1 Pavement model column

The model column consisted of soil samples and a concrete pavement slab retrieved from DFW airport that would replicate the airport pavement structure and subgrade. A specially designed wood box (0.61 m x 0.91 m x 0.91 m) was built for containing the pavement model using wood and Simpson Strong Ties on the inside corners for lateral reinforcement. Vertical joists were attached to the outside of the box for external reinforcement. Additional reinforcement was provided by placing rods of all thread at three levels of the box and prestressing them by tightening nuts on the outer ends.

Soil and concrete slab

Soil samples were collected from a site on DFW airport property. A total of 32 buckets of soil were collected. Representative samples were tested and classified according to American Society for Testing and Materials (ASTM) standards. The results of the dry sieve analysis (ASTM D6913) were misleading so a wet sieve analysis (ASTM D1140-17) was performed. The results from the wet sieve analysis reported 57.07% fines in the soil. Atterberg Limit tests (ASTM D4318-17) yielded liquid limit of 45, plastic limit of 25, and a plastic index of 20. Specific gravity of the samples was also tested (ASTM D854-14), with a result of 2.61. The resulting classification of the soil was CL-sandy lean clay.

A standard proctor test for compaction (ASTM D698) was performed to determine the maximum dry density and optimum moisture content of the soil. The maximum dry density was reported as 14.78 kN/m^{3,} and the optimum moisture content was 25% (Figure 1).

The soil samples were weighed and placed in a specially designed soil wetting box where water was added to achieve the desired moisture content of 20%. The column was filled at 15 cm lifts and compacted using a hand compactor. The moist density of the compacted soil was 13.78 kN/m^3, about 78% of maximum dry density, for the ease of compaction. Sensors were installed at various locations during the compaction process. Details of the sensors and their locations are discussed in the instrumentation section. A layer of fine sand approximately 25 cm in thickness was placed on top of the column to ensure a smooth interface between the sandy lean clay and the bottom of the slabs.

A sample of runway slab provided by the DFW Airport was used for the pavement. Thermal conductivity tests were conducted on the slab using the KD2 Pro manufactured by Decagon Devices, Inc. Two holes were drilled into the slab and filled with thermal paste to assist with the readings. The average thermal conductivity of the pavement slab was 2.74 W/m K. The slab was cut into two pieces with grooves cut into the faces for easier installation of instrumentation in the slab body. The slab halves were modified by grinding down high spots and filling low spots with commercial mason mix to achieve a smooth mating surface. Six holes were drilled into the grooves at a depth of 2 cm to accommodate the sensor heads of thermistors (Figure 2a, b). The gap around the sensor heads was then filled with commercial mason mix.

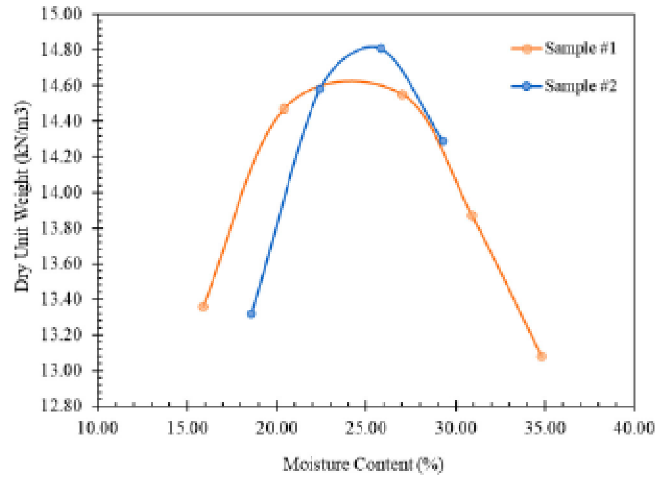

Figure 1. Standard Proctor compaction curve.

Assembly of the pavement column

The two slab pieces were placed on top of the soil using an overhead crane. The slab along with the box were moved into a freezer box using a forklift. Inside the freezer box, the gap between the two slab pieces was filled with the same commercial mason mix used to fill the gap around the sensor heads in the slab body. After baseline testing, the cooling and warming in the body of the slab was found to be uniform, confirming that the mason mix did not have an impact on temperature. The box was wrapped in R30 insulation and heavy-duty plastic wrap. The perimeter of the slab was also wrapped in R30 insulation, covered with a blue tarp, and sealed with silicone and Gorilla Glue to prevent water infiltration during misting operations. R30 insulation material was used to fill the gap between the box and the floor. The surface thermocouples were also installed at this time (Figure 3a through 3e).

Two misting systems were created to simulate precipitation events. The first system provided a faster rate of discharge of approximately 0.008 m^3/min. and was fabricated using landscape-grade nozzles attached to a hose with brass fittings (Figure 4a). The misting system was hung on the wall next to the soil column. The end of the hose was connected to an outside water reservoir through an access hole in the freezer wall, which was later sealed with foam insulation. The second misting system was used to simulate a low rainfall intensity and was fabricated using a patio misting system with smaller nozzles and a discharge rate of approximately 0.001 m^3/min. This system was hung directly over the soil column (Figure 4b).

2.2 Instrumentation

To monitor the temperature in the soil column and pavement slab, thermistors Type YSI 4404 (± 0.2 °C accuracy) manufactured by GeoKon were used. Thermistors were installed in

(a) (b)

Figure 2. (a): Slab after repair (b): Drilling holes for sensor heads.

various locations throughout the soil column to monitor the boundary conditions between the ambient freezer box temperature, the column, and the soil. Thermistors were also installed in locations to monitor the lateral and vertical temperature distribution throughout the soil column. To monitor the boundary condition at the interface of the soil and slab, an additional thermistor was installed in the fine layer of sand between the soil column and the slab. The locations and thermistors installed inside the soil are shown in Figure 5.

Six thermistors were installed in the body of the slab at a depth of 2, 25, and 48 cm. The sensors were oriented in two vertical rows of three to monitor the temperature distribution in the vertical and horizontal direction. Three Type T thermocouples (±0.5 °C accuracy) manufactured by National Instruments were installed on the surface of the slab at the center, edge, and between the center and edge. The center sensor was placed directly over a row of thermistors in the body of the slab to monitor the vertical temperature distribution throughout the entirety of the slab (Figure 6).

Two TDT SDI-12 temperature and moisture sensors (± 1 °C, ± 2% volumetric water content accuracy) manufactured by Acclima, Inc. were installed in the soil column to monitor the volumetric water content. The sensors were installed near thermistors to confirm that the thermistors were reading correctly (Figure 5). To monitor the ambient conditions in the freezer box, an EE181-L air temperature and relative humidity sensor (± 0.2 °C, ± (1.3 + 0.003*RH reading)% accuracy) manufactured by Campbell Scientific was used. A CR 1000x data logger from Campbell Scientific and a DataSnap SDI-12 logger from Acclima, Inc. were used for data acquisition.

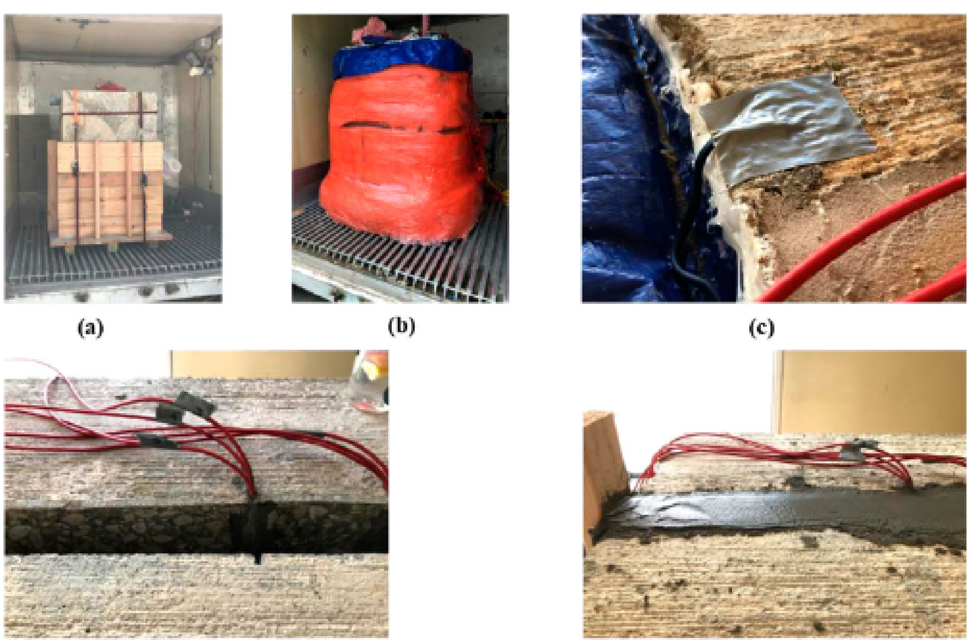

(d) (e)

Figure 3. (a): Complete system installed in the freezer box (b): Insulation wrapping (c): Installation of edge surface thermocouple (d): Gap between the slabs prior to filling (e): Gap after filling.

(a) (b)

Figure 4. (a): Insulated and wrapped pavement column with original misting nozzle head (b): Modified misting system.

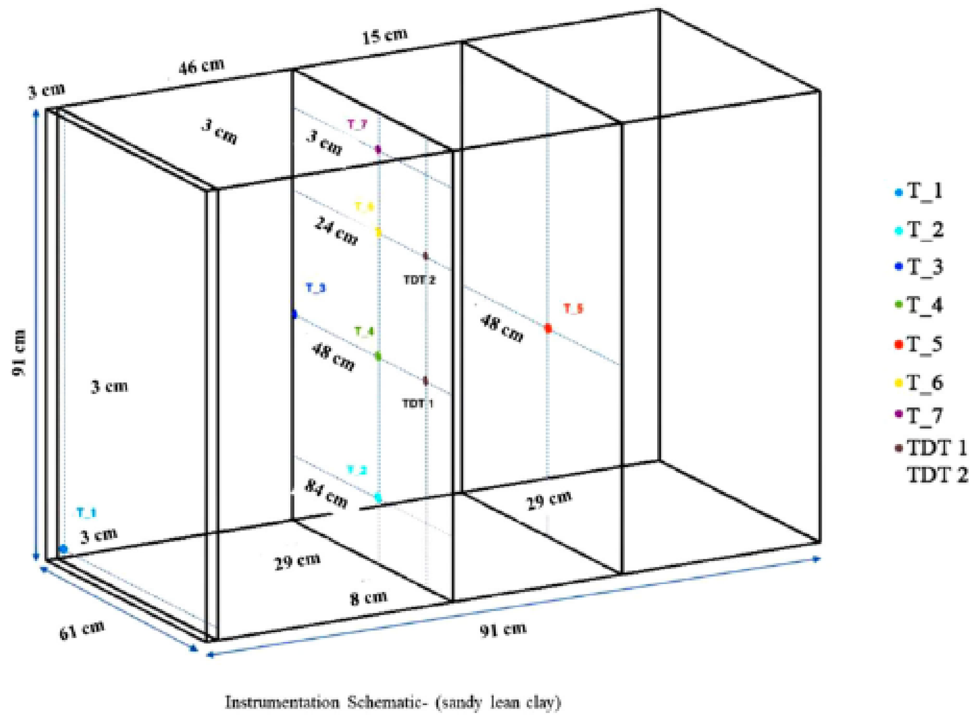

Figure 5. Soil instrumentation schematic.

2.3 Pavement icing test program

A baseline test was first performed to validate the function of the data acquisition system and obtain a baseline temperature response of the pavement column. Three cooling and misting tests were performed, namely cases 1, 2, and 3, to simulate typical weather scenarios observed from field weather data obtained from the DFW airport. A table summarizing the procedures for each test can be found in Table 1. Case 1 test involved a gradual temperature decrease from 4.4 °C to −3.9 °C over 84 h, with misting occurring when the slab surface reached −1.1 °C. Case 2 test involved a sharp temperature decrease from 4.4 °C to −9.4 °C over 24.5 h with misting occurring when the slab surface reached −1.1 °C. Case 3 test involved an actual cold front scenario, which occurred during the testing. Case 3 test was performed by opening the freezer box door to allow the outside air to influence the freezer box environment. This test was performed during a cold front experienced in Texas, with misting occurring when the slab surface reached 0 °C.

3 Baseline Cooling and warming tests

3.1 Baseline cooling test

Two baseline tests were performed to verify the pavement column temperature response to cooling and warming. The baseline cooling test was performed to obtain a baseline for the system as well as to confirm that the sensors and dataloggers functioned correctly. The freezer box was set to 15.6 °C and allowed to remain there for several days for the pavement

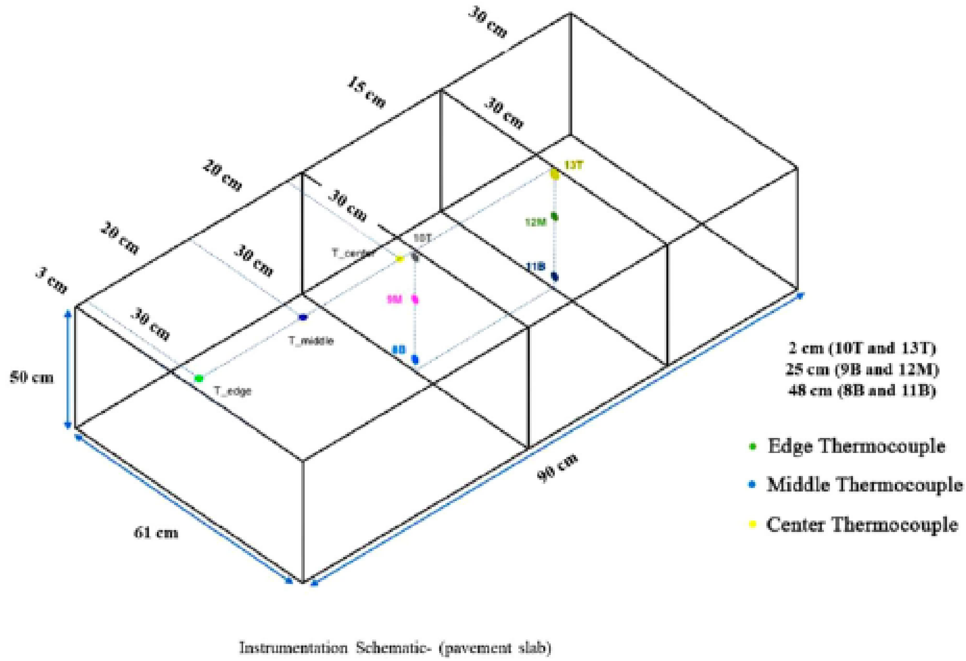

Figure 6. Pavement instrumentation schematic.

column to reach a steady state. The freezer box was then set to −6.7 °C where it remained for four days. Please note that the spikes in the ambient temperature on the plots are due to the defrost cycle in the freezer box. The thermistor data contained in the plots was processed using nine-point average in order to reduce the noise of the raw data. The slab temperature is plotted in Figure 7. The locations of the slab body sensors are: 2, 25, and 48 cm from the slab surface. Note that 'rt' in the plot legend refers to the right portion of the slab. Cooling of the slab surface is uniform; however, there is a difference in the temperature of the slab body and the ambient freezer temperature. The slab temperature is 2 °C to 6 °C warmer than the ambient air, even after being exposed to below freezing conditions for 89 h. The entirety of the slab body did not reach freezing despite the extended period of time in below-freezing conditions. This indicates that the soil is retaining heat and preventing the slab from freezing.

Figure 8 illustrates the lateral variation of the soil temperature at 98 cm below the slab surface. The three sensor locations can be seen in Figure 5. The soil has uniform temperature at the same depth, and the pavement column is under a 1-D heat transfer condition. It should be noted that sensor T_3 is located at the interface of the column wall and the soil. The plot shows that despite being at the boundary condition, T_3 does not have a discernible temperature variation compared to the others in the layer. This shows that the R30 insulation wrapping around the box is effective.

The vertical temperature profile in Figure 9 shows the temperature variation throughout the test in 24-hour increments. The pavement column had a uniform temperature

Table 1. Table of the testing program.

Test Name	Test Description
Baseline Cooling	The freezer start temperature was 15.6 °C, the freezer was set to −6.7 °C where it remained for 96 h.
Baseline Warming	The freezer start temperature was 2.8 °C; the freezer was then turned off and warming was controlled by outside air temperature for 145 h.
Case 1	Gradual temperature decrease from 4.4 °C to −3.9 °C over 84 h, with 38-minute misting using the first misting system occurring when the slab surface reached −1.1 °C. Temperature of mist was 0 °C.
Case 2	Sharp temperature decrease from 4.4°C to −9.4°C over 24.5 h, with 27.5-minute misting using the first misting system occurring when the slab surface reached −1.1 °C. Temperature of mist was 0 °C.
Case 3	The freezer box door opened during a cold snap to allow for the outside air to cool the pavement column. Outside temperature at the start of the test: 0 °C. Outside temperature at the end of the test: −3.3 °C. Misting occurred when the slab surface reached 0 °C, duration of misting using the second misting system was 21 min. Temperature of mist was 0 °C.

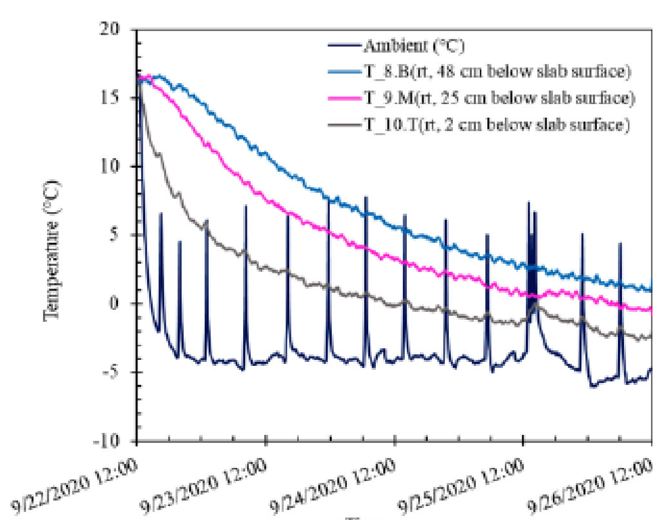

Figure 7. Variation of ambient freezer temperature and pavement slab.

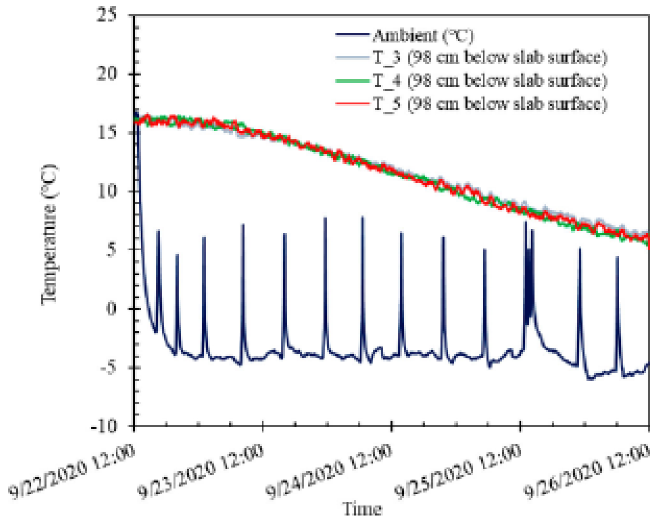

Figure 8. Variation of ambient freezer temperature and lateral soil temperature variation at 98 cm below the slab surface.

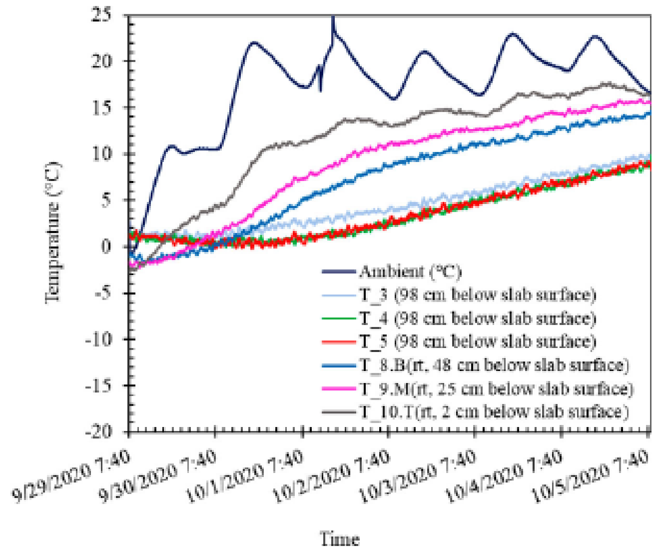

Figure 10. Variation of ambient freezer temperature and pavement slab and horizontal soil layer 98 cm below slab surface.

profile, in equilibrium with the air temperature, when the test began. By the end of the test, the slab temperature decreased by 17 °C and the soil at 98 cm below the slab surface decreased by 12 °C. The depth of maximum temperature was found between 70 and 100 cm below the slab surface. The maximum temperature depth is increased with increase of time, which represents typical pavement temperature profiles in the field. The baseline cooling test was repeated and the same cooling trends were observed for the second test.

3.2 Baseline warming test

This test was performed to obtain a warming baseline for the system. The freezer box was 2.8 °C when it was turned off and allowed to be warmed by the outside air with average daily temperature of 21.1 °C for six days. Figure 10 shows the slab and ambient temperature as well as the temperature of the soil at the mid-depth (98 cm below the slab surface). The slab follows the general warming trend of the ambient air, but there is a significant temperature difference between them. The slab temperature does not begin to converge with the ambient temperature until the end of the six-day test. The soil mid-depth increases in temperature by 8 °C. This shows that the insulation is effective. The vertical temperature profile shown in Figure 11 illustrates the temperature change of the system in 24-hour increments. From the plot, the slab is approximately 6 °C warmer than the soil at mid-depth. The soil at 10 cm to 70 cm distance to the base of the column first released heat to its surrounding soils before it started absorbing heat. A TDT moisture sensor was installed in the same lift as T_3, T_4, and T_5 (98 cm below the slab surface) in the soil. Figure 12 shows the volumetric moisture content of the the soil, in percent, as well as the temperature of the soil. The moisture in the soil shows little variation throughout the testing period, illustrating that the plastic wrapping and sealing of the slab edges was effective in preventing water infiltration during the misting operations. The temperature readings from the TDT sensor agree with the readings from the thermistors T_3, T_4, and T_5, indicating that all of the sensors were working correctly.

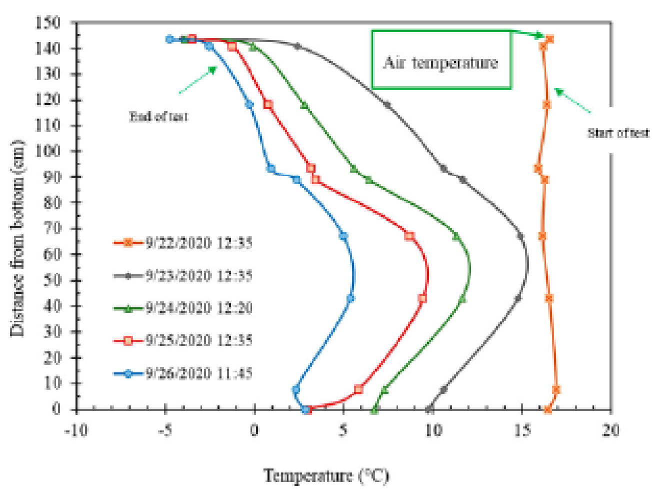

Figure 9. Vertical profile of temperature variation in the system (24-hour increments).

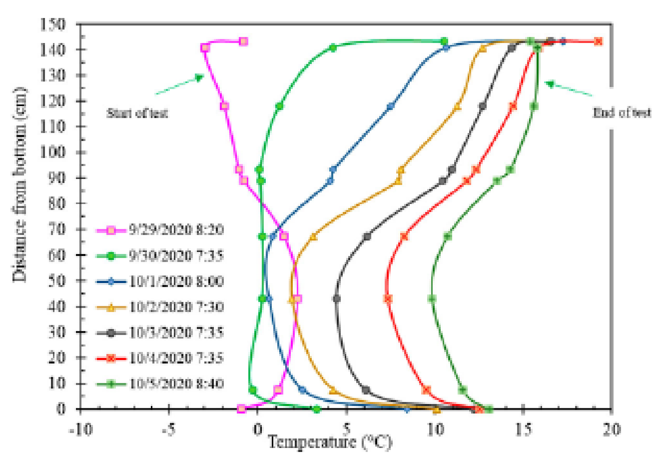

Figure 11. Vertical profile of temperature variation in the pavement column (24-hour increments).

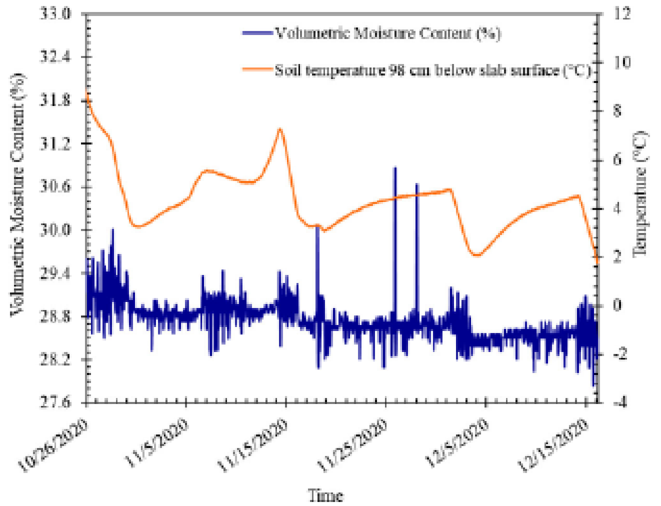

Figure 12. Volumetric moisture content (%) and temperature (°C) of soil at 98 cm below slab surface.

4 Results and discussion

The next section presents the results of the test cases, a summary table of the results can be found below in Table 2. The location for the sensors noted in Table 2 can be found in Figures 5 and 6.

4.1 Gradual temperature decrease (Case 1)

The scenario for case 1 is a gradual decrease from 4.4 °C to −3.9 °C over 84 h. The freezer box temperature was decreased incrementally until reaching −3.9 °C, where it remained for an additional 10 h, at which time the misting operation began. Based on previous tests, it was observed that the slab surface does not respond immediately to a change in ambient freezer air temperature. During this test it was observed that the air in the freezer box took 48 h to reach −0.6 °C, but the surface of the slab took an additional 36 h to reach 0 °C. Hence, extra time was allotted before beginning the misting operation. The surface temperature of the slab was −1.1 °C and the ambient temperature in the freezer box was −3.4 °C at the start of the misting operation. The second misting system simulating a low-intensity rainfall was used in this test. The finer mist allowed for more even coverage over the surface of the pavement. The temperature of the water used for misting was monitored with a thermistor. The temperature of the water during misting was 0 °C and the duration of the misting operation was 38 min at a discharge rate of approximately 0.001 m^3/min. Figure 13 shows the variation in the ambient freezer temperature, the slab surface, and the slab body. While the slab surface follows the ambient temperature, the slab body temperature decreases at a slower rate. Sensor T_10 (2 cm below slab surface) follows the center surface sensor closely with a slightly higher temperature. Sensors T_8 and T_9 (25 and 48 cm below slab surface, respectively) are warmer than the surface and T_10 sensors. It is important to note that freezing temperatures were not recorded deeper into the slab body, despite the extended time in freezing conditions. This can be attributed to the thermal capacity of the slab as well as the soil beneath it. Figure 13 also shows the temperature decrease of the soil at mid-depth (98 cm below slab surface) and at the soil/slab interface (52 cm below slab surface). The soil layer at the slab-soil interface cooled at a more rapid rate than the mid-depth layer. Neither soil layer reached freezing temperatures despite being in freezing conditions for 52 h. This illustrates the significance of the thermal capacity of the subsurface. Through real-time video and analysis of time stamp photographs taken during the misting operation (Figure 14), the formation of ice was observed 12 min after the start of misting with a discharge rate of approximately 0.001 m^3/min.

Table 2. Summary of test results.

	Measured Data	Initial Conditions (°C)	Final Conditions (°C)	Temperature Change (°C)	Rate of Change (per hour)
Baseline Cooling Case (96 h)	Ambient	20.4	−4.6	−25	−0.26
	Slab Body (8B)	16.6	−0.3	−16.9	−0.18
	Soil (T4 and T5)	16.4	4.1	−12.3	−0.13
Baseline Warming Case (145 h)	Ambient	2.8	15.4	+12.6	+0.28
	Slab Body (8B)	−2.3	15.2	+17.5	+0.39
	Soil (T4 and T5)	0.3	11	+10.7	+0.24
Gradual Temperature Decrease (84 h)	Ambient	4.4	-3.9	−8.3	−0.10
	Slab Surface	8.8	−0.1	−8.9	−0.10
	Slab Body (8B)	11.1	1.3	−9.8	−0.12
	Soil (T4 and T5)	7.3	4.1	−3.2	−0.04
	Due to the surface being exposed to freezing conditions for such a long duration, the ambient temperature overcomes the soil's influence on the surface. The formation of glaze is observed 12 min after the beginning of the misting operation.				
Rapid Temperature Decrease (49 h)	Ambient	5.1	−9.2	−14.3	−0.29
	Slab Surface	5.2	−6.6	−11.8	−0.24
	Slab Body (8B)	5.2	1.5	−3.7	−0.08
	Soil (T4 and T5)	4.6	−3.1	−7.7	−0.16
	The ambient air has more of an effect on the slab temperature, due to the longer duration of cold temperature exposure. The formation of ice is observed 19 min after the beginning of the misting operation.				
Natural Temperature Decrease (46 h)	Ambient	4	−2.9	−6.9	−0.15
	Slab Surface	4.4	0	−4.4	−0.10
	Slab Body (8B)	3.2	0	−3.2	−0.07
	Soil (T4 and T5)	0.1	−0.3	−0.4	−0.01
	During the test, the soil response to the decrease in temperature is negligible, illustrating the influence of the soil's thermal capacity on its response. This influence can also be observed when considering the difference in the change between the ambient temperature and the slab temperature. Ice formation is observed 10 min after the start of the misting operation, with the layer continuing to thicken throughout the remaining duration of the test.				

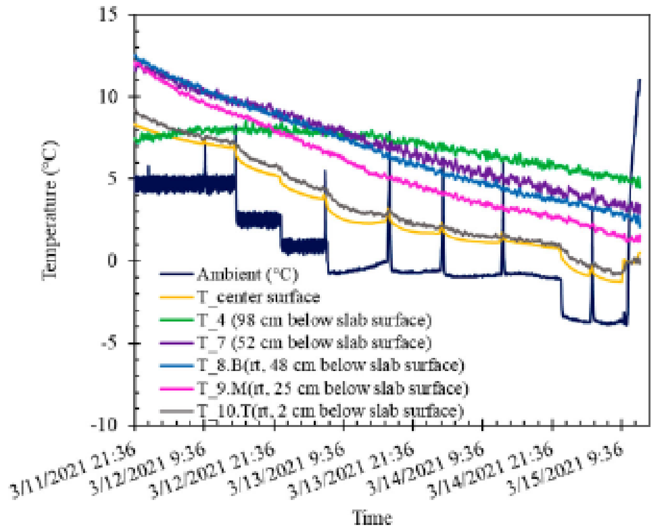

Figure 13. Variation of ambient freezer temperature, slab surface, slab body, soil at mid-depth (98 cm below slab surface), and slab/soil interface (52 cm below slab surface).

Figure 14 shows the final slab condition. Due to the very fine mist and the slower rate of droplet deposit onto the surface, the formation of a thin glaze of ice is observed 12 min after the start of the misting. This glaze is similar to the icing glaze that forms during a freezing rain, drizzle, or fog event.

4.2 Rapid temperature decrease (Case 2)

During this test, the temperature in the freezer box was decreased quickly from 4.4 °C to a final temperature of −3.9 °C, where it remained for 24.5 h before the misting operation began. The additional time was allowed for the slab surface to reach freezing conditions before misting began. The temperature of the slab surface was −2.2 °C and the ambient temperature was −4.2 °C at the start of the misting operation. The temperature of the water used for misting was monitored with a thermistor. The temperature of the water during misting was 0 °C, misting was 27.5 min in duration using the first misting system with a faster rate of discharge of approximately 0.008 m^3/min. The formation of ice was observed approximately 19 min after the start of misting. Figure 15 shows the time lag between the ambient temperature, slab surface, and slab body throughout the test. From Figure 15, it can be observed that the sensor located on the edge of the surface follows the temperature profile of the ambient temperature much closer than the sensors at the center of the slab surface. This indicates that the edge is more responsive to changes in the surrounding outside environment rather than the internal slab or soil temperature. The vertical temperature profile in Figure 16 illustrates how after being at a freezer box setting of −9.4 °C for 12 h, the temperature of the slab decreases by approximately three degrees while the soil decreases by two degrees.

Figure 17 shows the final slab condition. The formation of ice was observed 19 min after the start of the misting operation with a discharge of approximately 0.008 m^3/min. The ice coating was non-uniform with the thickest ice forming on the surface closest to the misting nozzles. As the distance from the nozzles increased, the surface ice decreased in thickness and occurrence. The circled portion in Figure 17a indicates the ice formation on the side of the slab that was close to the misting nozzle. As indicated in the photo, the ice is fairly consistent in this location, where further away from this area there is little to no ice formation. Figure 17b shows a thick layer of ice formation, this occurred very close to the nozzle location. This test was repeated and yielded similar results and ice formation patterns.

4.3 Temperature decrease due to natural conditions (Case 3)

During the case 3 test, one freezer door was opened slightly to allow the cold outside air to influence the ambient temperature of the freezer box to create a field-like condition. The door remained opened for a period of approximately 45 h before misting began. The outside air temperature was 0 °C at the start of the test and −3.3 °C at the end. When misting began the temperature of the water was 0 °C, the ambient temperature of the freezer box was −3 °C and the slab surface was −0.6 °C. The duration of the misting operation was 21 min using the second misting system with a slower discharge rate of approximately 0.001 m^3/min. Results from this test show that it took the slab surface an additional 24 h to reach 0 °C after the ambient temperature in the freezer box had reached below freezing temperatures. Even after 24 h, the surface just barely goes below freezing. Figure 18 shows the variation

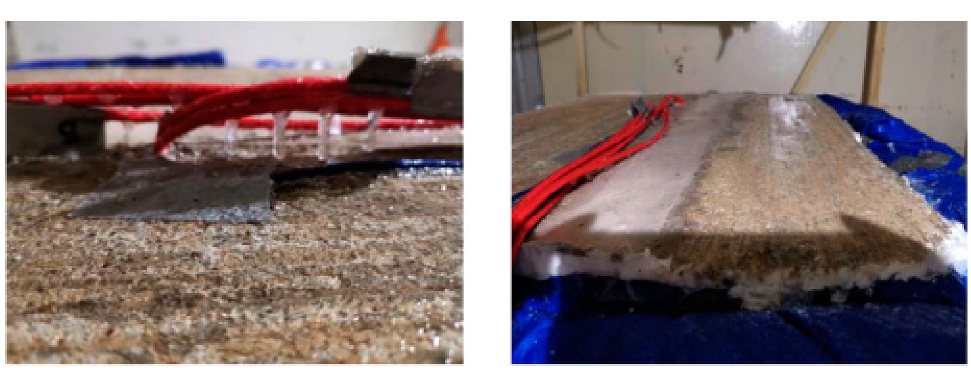

Figure 14. Final slab condition showing the formation of glaze.

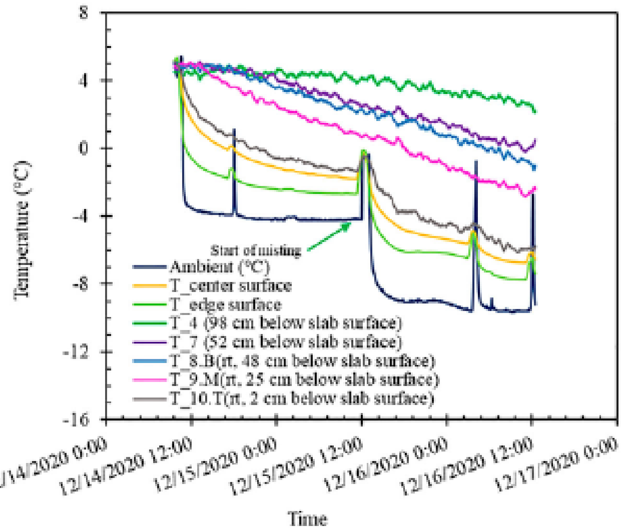

Figure 15. Variation of ambient freezer temperature, slab surface, and slab body.

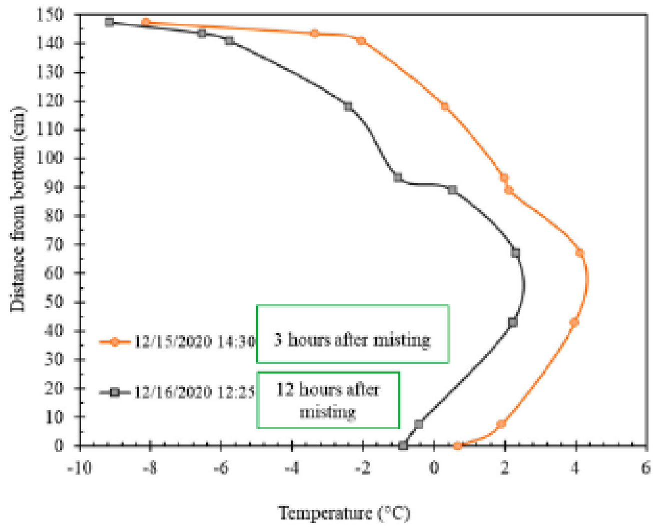

Figure 16. Vertical profile of temperature variation in the system.

between the outside temperature, the ambient freezer box temperature, and the slab. The surface sensor and T_10 (2 cm below slab surface) follow the ambient temperature. Deeper into the body of the slab, there is not a significant

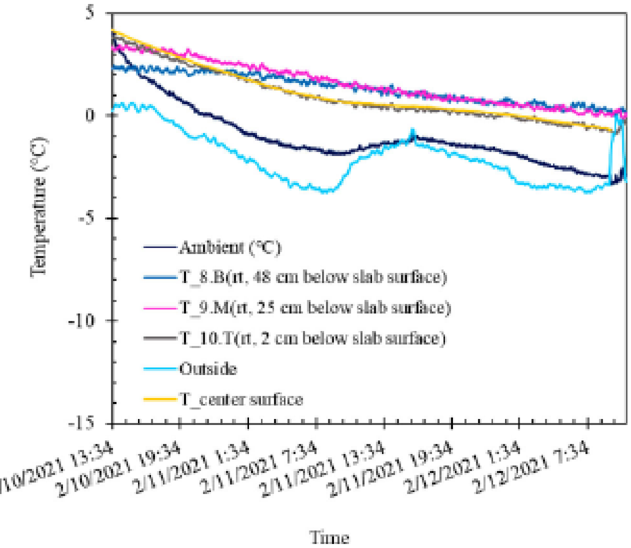

Figure 18. Variation of outside temperature, ambient freezer temperature, slab surface, and slab body.

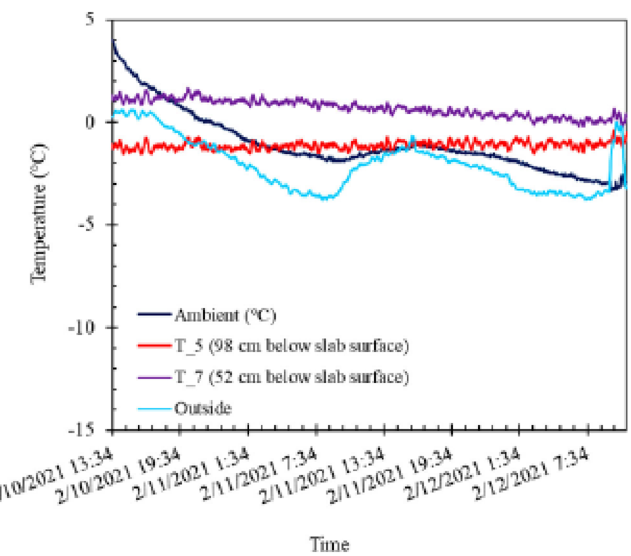

Figure 19. Variation of outside temperature, ambient freezer temperature, the soil at mid-depth (98 cm below slab surface), and slab/soil interface (52 cm below slab surface).

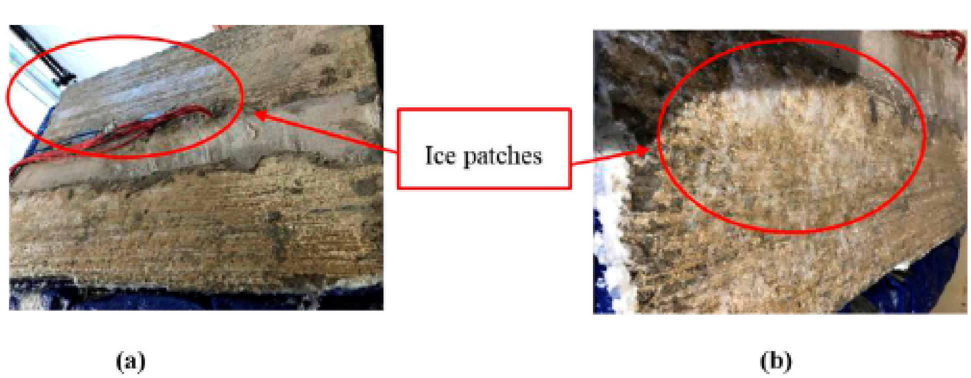

Figure 17. (a): Ice formation on the slab surface (b): Thicker ice formation closer to the misting nozzle.

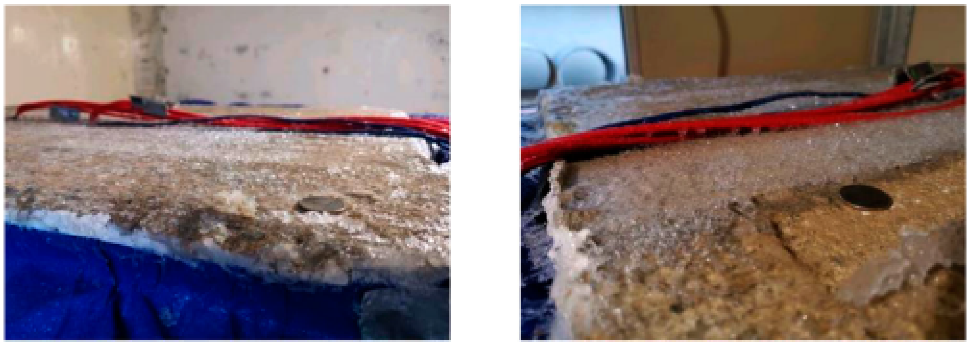

Figure 20. Final slab condition with ice formation on slab surface after misting.

temperature decrease and the body of the slab did not reach freezing conditions at any point during the 46-hour test. Figure 19 shows the soil temperature at mid-depth (98 cm below slab surface) as well as the temperature at the soil/slab interface (52 cm below slab surface). Both layers do not experience any significant temperature change. This can be attributed to the thermal capacity of the soil preventing any appreciable temperature decrease. Ice formation was observed 10 min after misting began, with the ice continuing to solidify after misting ended. Due to the slower rate of discharge, the layer of ice was thick and uniform throughout the slab surface (Figure 20).

4.4 Prediction of surface temperature

SUPERPAVE® Mix Design System is the design software used to choose the appropriate asphalt binder for a pavement design based on weather conditions (Huber 1994). The empirical equation used in this study is based on an equation in the SUPERPAVE® software that relates the temperature at a specific depth to the temperature of the pavement surface. A limitation of the equation used is that there are not any terms to account for the effects of radiation on the net heat flow at the pavement surface. This equation was chosen due

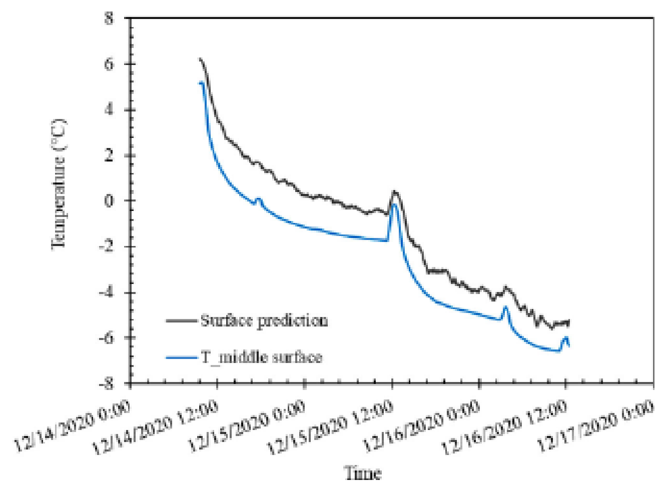

Figure 22. Comparison of surface temperature prediction and measured surface temperature for case 2 (rapid temperature decrease).

to the lack of radiation effects in this study because the system was installed into the freezer box.

$$T_s = \frac{T_{20} + 0.80899}{0.9545} \tag{1}$$

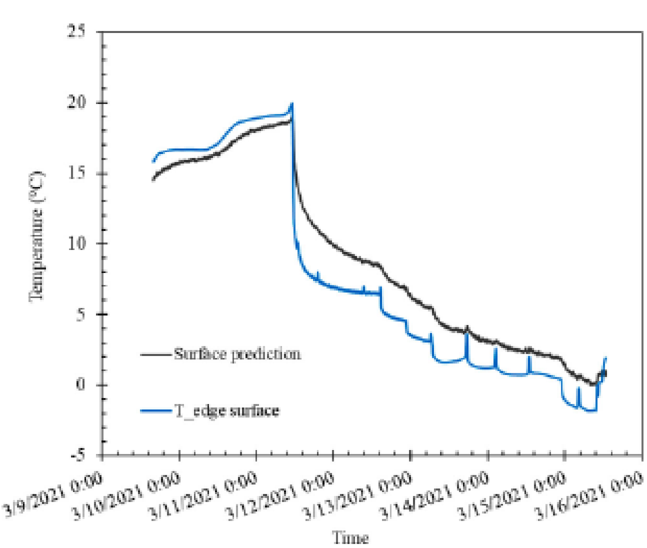

Figure 21. Comparison of surface temperature prediction and measured surface temperature for case 1 (gradual temperature decrease).

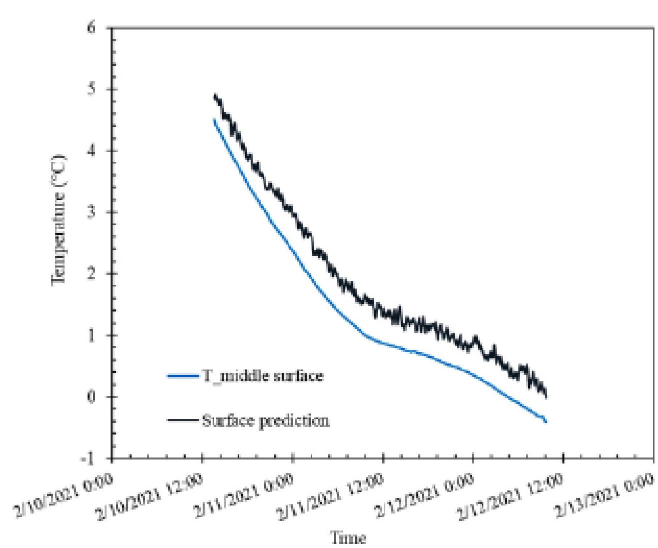

Figure 23. Comparison of surface temperature prediction and measured surface temperature for case 3 (natural conditions).

where T_s is the surface temperature and T_{20} is the temperature at a depth of 20 mm, both are in °C. The sensor used for T_{20} is T_10 which is 19 mm below the slab surface. Figures 21–23 compare the predicted surface temperature and the measured surface temperature for the three test cases.

5 Conclusions

This study presents a series of controlled tests performed using a model column in a freezer box to explore the time and conditions required for the formation of ice to occur during a precipitation event. The pavement and the sub-soil exhibited a delayed response to the simulated cold fronts. Analysis of the subsurface conditions show that the soil's response to cold fronts is not immediately apparent and is minimal. The results show that the subsurface exerts some influence on the behavior of the pavement slab, but the ambient temperature of the freezer box is the more dominant factor. The difference in the rate of change in the model's temperature can be attributed to the thermal inertia of both the pavement and the soil beneath it. The formation of ice is mainly governed by the pavement surface temperature and the moisture duration and intensity, it is not dependent on the rate of ambient temperature decrease. For the case of a gradual temperature decrease, the formation of ice was observed 12 min after the start of misting. The rapid temperature decrease case resulted in the formation of ice being observed 19 min after the start of misting. The formation of ice occurring earlier during the gradual temperature decrease can be attributed to the use of the second misting system which had a slower rate of discharge than the first misting system and distributed water more evenly during misting. For the case of natural temperature decrease, the formation of ice was observed 10 min after the start of misting. The faster rate of ice formation here can be attributed to the freezer box door being open during misting, allowing the wind from the outside to influence the conditions inside the freezer box. However, more studies are needed to determine the effects of wind on the formation of surface ice.

Acknowledgements

This research is supported by Dallas Fort-Worth International Airport. The authors appreciate the assistance provided by the program manager Eduardo Tovar and his office. The assistance of Nice Kaneza, Dr. Teng Li, and Vishal Kothari during the study is greatly appreciated.

Disclosure statement

No potential conflict of interest was reported by the author(s).

References

Chen, J., Wang, H., and Xie, P, 2019. Pavement temperature prediction: theoretical models and critical affecting factors. *Applied Thermal Engineering*, 158.

Dai, H., et al., 2012. Evaluation on the effects of deicing chemicals on soil and water environment. *Procedia Environmental Sciences*, 2122–2130. doi:10.1016/j.proenv.2012.01.201

Huber, G. A, 1994. *Weather database for the SUPERPAVE mix design system*. Washington, DC: National Academy of Sciences.

O'Keefe, K., and Shi, X, 2005. *Synthesis of information on anti-icing and Pre-wetting for winter Highway maintenance practice in North America*. Bozeman: Western Transportation Institute.

Qiu, X., Xu, J., and Yang, Q, 2018. Asphalt pavement icing condition criterion and SVM-based prediction analysis. *J. Highway Transp. Res. Dev. (English Ed.) (Journal of Highway and Transportation Research and Development (English Edition))*, 1–9. doi:10.1061/JHTRCQ.0000647

Snow & Ice- FHWA Road Weather Managment, 2020, February 20. Federal highway administration: https://ops.fhwa.dot.gov/weather/weather_events/snow_ice.htm.

Sutter, L., et al., 2006. Long-Term effects of magnesium chloride and other concentrated salt solutions on pavement and structural portland cement concrete. *Transportation Research Record*, 60–68. doi:10.1177/0361198106197900109

Usman, T., Fu, L., and Miranda-Moreno, L. F, 2012. Quantifying safety benefit of winter road maintenance: accident frequency modeling. *Accident Analysis & Prevention*, 42 (6), 1878–1887. doi:https://doi.org/10.1016/j.aap.2010.05.008

Veneziano, D., Shi, X., and Fay, L., 2018. Economic benfits of winter road operations. *Sustainable Winter Road Operations*, 156. doi:10.1002/9781119185161.ch9

Zhao, X., Shen, A., and Ma, B, 2020. Temperature response of asphalt pavement to low temperatures and large temperature differences. *International Journal of Pavement Engineering*, 21 (1), 49–62. doi:10.1080/10298436.2018.1435883